Treatment of Intimal Hyperplasia with The Targeted Delivery of Lipid Nanoparticles *Ex Vivo*

Saba Niaz [1*], Guillaume Bastiat Partner [2*], Patrick Saulnier [2]

Abstract

Background: Lipid nanocapsules (LNCs) have gained attention as a promising strategy for developing innovative drug release systems aimed at treating intimal hyperplasia. These systems allow for the localized and sustained release of both hydrophilic and lipophilic drugs, while minimizing disruption to the normal healing process. Despite their potential, the pharmacological capabilities of LNCs in addressing cardiovascular pathologies remain underexplored. Methods: In this study, we investigated novel LNC formulations with varying surface properties by incorporating different concentrations of Span® 80. The aim was to assess the impact of these formulations on the interaction of LNCs with tissues. LNCs were characterized based on their average size, polydispersity index (pdI), and zeta potential, with Span compositions of 0, 0.14, and 0.27 (w/wLNC). Results: The characterization of LNCs revealed consistent and reproducible sizes, pdI values, and zeta potentials across all formulations. Ex vivo experiments demonstrated that the LNC formulation containing a Span composition of 0.27 (w/wLNC) showed the fastest and highest levels of interaction with tissues throughout the incubation period. Conclusion: The study highlights the potential of LNCs with tailored surface properties as a significant advancement in targeted drug delivery for cardiovascular pathologies. The findings suggest that such formulations can offer reduced toxicity and precise control over drug release kinetics, paving the way for optimized therapeutic efficacy and minimized adverse effects. Continued research in this area could lead to transformative treatments for intimal hyperplasia and related conditions.

Keywords: Intimal Hyperplasia, Lipid Nanocapsules, Vascular Smooth Muscle Cells, Targeted Drug Delivery, Span 80, ex vivo blood vessels

Significance | This study demonstrated lipid nanocapsules' potential to improve targeted drug delivery in treating intimal hyperplasia, reducing restenosis risk.

*Correspondence. Saba Niaz, Imperial College London, UK
E-mail: niazsaba274@gmail.com

Editor Md Shamsuddin Sultan Khan, And accepted by the Editorial Board Mar 25, 2024 (received for review Jan 22, 2024)

Introduction

A peripheral vascular disorder called intimal hyperplasia (IH) causes the thickening of the artery wall away from the coronary and cerebral circulation, ultimately resulting in diminished organ perfusion. Over 40% of all cardiovascular disorders globally are caused by IH, making it the most common cardiovascular condition (Fowkes et al., 2013). IH initially manifests as a physiologic healing reaction to a blood vessel wall injury (Nemenoff et al., 2008). It is generally known which cell types are involved in the restenotic process. There are three important layers in a healthy blood vessel. The innermost layer, known as the tunica intima or intimal layer, comes into contact with the blood that is coursing through the artery. Endothelial cells make up the majority of cells in this stratum. The tunica media, also known as the medial layer, is located next to the intimal layer and is predominantly made up of smooth muscle cells. The tone of the blood vessels is controlled by this layer. The tunica adventitia, also known as the adventitial layer, is the skin's outermost layer and provides structure and elasticity (Bhargava et al., 2006).

Author Affiliation.
[1] Imperial College London, UK
[2] Université d'Angers, Inserm, CNRS, MINT, SFR ICAT, Angers, France

Please cite this article:
Saba Niaz, Guillaume Bastiat Partner et al. (2024). Treatment of Intimal Hyperplasia with The Targeted Delivery of Lipid Nanoparticles Ex Vivo, Biosensors and Nanotheranostics, 3(1), 1-8, 7338

A variety of cellular and extracellular events control the multifactorial process of IH. A cascade of processes involving cells and tissues present at the damage site begins because of vascular injury, which is unavoidable during vascular interventions (Melnik et al., 2022). Endothelial cell (EC) damage is the first step in the development of IH. The EC serves as the blood-vessel wall interface, preventing thrombus formation and controlling vascular tone (vasodilation and vasoconstriction). Following surgery, EC loss encourages platelet aggregation, inflammatory cell recruitment/activation, and vasoconstriction. The "activated" EC, attracted platelets, and immune cells, which release cytokines and chemokines that cause an inflammatory reaction (Mylonaki et al., 2018).

Additionally, vascular smooth muscle cells (VSMCs) and fibroblasts are stimulated by growth factors secreted by these cells, such as platelet-derived growth factor (PDGF), basic fibroblast growth factor (bFGF), transforming growth factor-beta 1 (TGF-β1), and thromboxane A2. Nitric oxide (NO) and hydrogen sulfide (H2S), EC-derived gasotransmitters, are lost when these substances are secreted, which together stimulate vascular remodeling and reprogramming of cells in the media and adventitia layers. This injury-induced phenotypic modulation of VSMCs promotes repair of the lesion, but failure to resolve the healing response leads to the formation of a neointima layer between the intima and the internal elastic lamina. This new layer is made of VSMC-like cells and an extracellular matrix (ECM) (Chakraborty et al., 2021; Déglise et al., 2022). In response to injury, VSMCs continue to have the capacity to move and divide quickly. A transformation in the spectrum of activated genes, commonly referred to as "phenotypic modulation," is naturally necessary for such a change in behavior and is a requirement for migration and proliferation. Peptides that bind to receptors with intrinsic tyrosine kinase activity are the most effective mitogens for VSMCs. These connect indirectly to several signaling pathways, including the phosphoinositide 3-kinase, protein kinase B route, the diacylglycerol, and protein kinase C pathways (Brito & Amiji, 2007).

To reduce restenosis in IH, many medications have been explored over the years. There are numerous approaches to treating restenosis. Drugs have been coated on mechanical stents that keep the vessel open to stop cells from encroaching on the vascular lumina. Anti-cancer and anti-inflammatory drugs have been utilized, among other pharmacological classes, to treat restenosis. Plasmid DNA and RNA interference have been used to modify genes to enhance or decrease the local concentrations of particular signaling molecules that are used to suppress the growth of some cells while stimulating the growth of other cells. Each of these treatments primarily aims to inhibit SMC proliferation while promoting the vessel's re-endothelialization, hence restoring the vessel's health (Farb et al., 2002).

Antiproliferative medications like paclitaxel, which prevent cell division, are successful in treating both cancer and neo-intimal hyperplasia, the primary factor in restenosis (Li et al., 2016). In-stent restenosis, which was formerly thought to be a serious negative effect of percutaneous coronary stent implantations, is now substantially less common because of drug-eluting stents. The key factor causing in-stent restenosis is the abnormal proliferation of vascular smooth muscle cells (VSMC), which is hindered by the localized release of antiproliferative medicines. Following balloon angioplasty, intimal hyperplasia is completely inhibited, and luminal constriction is prevented by the slow release of paclitaxel administered to the peri-vascular area (Bhargava et al., 2006).

To obtain desired therapeutic outcomes in the treatment of IH, both conventional medications and gene-based therapies have been delivered using nanoparticles. Since current therapies have drawbacks such as in-stent restenosis, drug-eluting stents (DES) related thrombosis development, and a high rate of restenosis with balloon angioplasty and bare metal stent use, there is a need for alternate therapy. Since local or targeted administration can be accomplished, lowering systemic toxicity while reaching particular cell types in adequate concentrations for the required duration of time, nanoparticle delivery systems are well-suited for the treatment of restenosis. Polymers and lipids that are biocompatible also don't cause an inflammatory reaction (Westedt et al., 2002).

Lipid nanocapsules (LNCs) are bioinspired nanocarriers whose structure is a cross between liposomes and polymeric nanoparticles. Medium-chain triglycerides make up the oily core of LNCs, which is encased in a surfactant shell (Matougui et al., 2016). LNCs are a well-established system and were first patented by Heurtault et al. (2002). LNCs serve as carriers for a variety of delivery methods, including oral, intravenous, pulmonary, and local delivery (Umerska et al., 2015). Small particle size (20–100 nm), strong physical stability, and manufacturability using the phase inversion temperature method, an organic solvent-free, low-energy process, are all benefits of LNCs. Due to their PEGylated shell and their versatility in terms of surface modifications, LNCs can provide an interesting platform for nanomedicine. The oily core of LNCs allows the easy incorporation of lipophilic dyes for labeling (Umerska et al., 2015; Huynh et al., 2009).

Since 2002, the LNCs' physical characteristics, including particle size and zeta potential, and biological characteristics have been thoroughly researched (Minkov et al., 2005; Hirsjärvi et al., 2012; Groo et al., 2018). LNCs share similarities with surface-active compounds in that they have both hydrophilic and hydrophobic components. They can be manufactured in a range of sizes to suit different purposes, and their properties can be considerably altered by altering their composition (Béduneau et al., 2007). Additionally, LNCs provide the ability to load pharmacological molecules that are both hydrophilic and hydrophobic. LNCs had previously been

investigated for their usefulness as drug delivery systems for treating disorders including cancer, antibiotic resistance, and ocular conditions, including age-related macular degeneration, because of their biomimetic nature (Groo et al., 2018; Urimi et al., 2021).

There is currently no established role for lipid nanocapsules in the treatment of intimal hyperplasia. However, some research has suggested that lipid-based nanocapsules, such as liposomes or solid lipid nanoparticles, could potentially be used to deliver drugs or therapeutic agents to the site of intimal hyperplasia. Moreover, it has been proposed that lipid nanocapsules could be used to deliver anti-proliferative agents, such as paclitaxel or siRNA, to the site of intimal hyperplasia to inhibit the proliferation of SMCs and reduce the development of intimal hyperplasia (Brito & Amiji, 2007).

The study aimed to explore the potential role of different LNC formulations with various Span® 80 compositions in the management of intimal hyperplasia, highlighting their ability by elucidating the mechanisms underlying the interaction between LNCs and the vascular wall of blood vessels and providing valuable insights into the development of LNC-based strategies for the prevention and treatment of intimal hyperplasia. Moreover, to assess the impact of LNCs loaded with fluorescence dye on internalization into blood vessel *ex vivo* tissues.

2 Materials and methods

2.1 Materials

Span® 80 (sorbitan monooleate) (Span), Kolliphor® HS15 (mixture of free polyethylene glycol 660 and polyethylene glycol 660 hydroxystearate) (Kol) were purchased from BASF (Ludwigshafen, Germany). Labrafac® WL 1349 (caprylic-capric acid triglycerides) (Lab) was provided by Gattefossé S.A. (Saint-Priest, France). NaCl was purchased from Prolabo (Fontenay-sous-bois, France). 1,1′-dioctadecyl-3,3,3′,3′-tetramethylindodicarbocyanine 4-chlorobenzenesulfonate (DiD) (lipophilic carbocyanine dye family) were provided by Molecular probes® (Eugene, OR USA). Deionized water was obtained from a Milli-Q plus® system (Millipore, Bilerica, USA).

2.2 Formulation of lipid nanocapsules (LNCs)

The lipid nanocapsules (LNCs) were prepared using the phase inversion temperature (PIT) approach. The LNC formulation followed a phase-inversion process, transforming from an oil-in-water emulsion at a low temperature to a water-in-oil emulsion at a high temperature. This process has been extensively described in previous studies [14]. The quantities of Labrafac (oil phase), water, NaCl (aqueous phase), Kol and Span (surfactants) were accurately measured for each formulation, as outlined in Table 1 for LNCs with Span compositions of 0, 0.14 and 0.27 (w/w_{LNC}).

To prepare the LNCs with different Span compositions (w/w_{LNC}) (0, 0.14 and 0.27), the following procedure was followed. Three cycles of heating and cooling were performed, alternating between temperatures of 90°C and 50°C. Throughout this process, all ingredients were continuously stirred using a magnetic stirrer at approximately 900 rpm. During the final cooling cycle, an irreversible thermal shock was induced by adding 2 mL of cold water (4°C), leading to the spontaneous formation of an LNC suspension. After the thermal shock, the LNC suspension was stirred continuously until it reached room temperature. The weight fractions of Span for different LNCs concentration (0,0.14 and 0.27), were calculated from the total weight of LNCs as followed:

$$\text{Span } (w/w_{LNC}) = \frac{\mathrm{m_{Span}}}{\mathrm{m_{Span}} + 0.7 \times \mathrm{m_{Kol}} + \mathrm{m_{Lab}}}$$

A factor of 0.7 was included in the calculation as only 70% of the Kol corresponds to surfactant (PEGylated hydroxystearate), while the remaining 30% corresponds to free PEG (data of the supplier).

To prepare fluorescent-labeled LNCs, DiD was dissolved in a solution of Lab at a concentration of 0.1% (w/w_{Lab}) thanks to the addition of acetone. After solubilization, the mixture was then subjected to magnetic stirring at 40°C for one night to facilitate the complete evaporation of acetone. Then, fluorescent-labeled LNCs, referred as DiD-labeled LNCs, with various Span compositions (0, 0.14, and 0.27) were created as described previously. The DiD was loaded into the oil phase in the core pf LNCs. It is important to note that these steps were carried out in a dark environment to minimize any potential light-induced effects.

2.3 Characterization of size distribution and Zeta potential of LNCs

Using a Zetasizer® Nano ZS (Malvern Panalytical, United Kingdom), the size distribution, including hydrodynamic diameter (Z-ave) and polydispersity index (PdI), and the zeta potential (ZP), of both LNC suspensions and fluorescent-labeled LNCs were measured. The 4-mW Helium-Neon laser in the quasi-elastic light scattering device has a fixed scatter angle of 173° and an output wavelength of 633 nm. For the Z-ave and PdI measurements, the correlation functions were fitted using an exponential fit (Cumulant method). The electrophoretic mobility necessary for ZP determination was calculated using the Smoluchowski approximation. The size measurement was performed after diluting the LNCs suspension by a factor of 60, respectively, in Milli-Q water at 25°C.

2.4 LNC incubations with blood vessel ex vivo tissue

To assess the interaction of DiD-labeled LNCs with different Span compositions (0, 0.14 and 0.27) with tissues, firstly, blood vessel *ex vivo* tissues were obtained from CarME laboratory (UMR Inserm U1083 / CNRS 6015, University of Angers) from animal models (rats and mice). The blood vessel tissues were transferred into Eppendorf tubes containing 500 µL of the DiD-loaded LNC suspension (10 mg/mL) prepared in 1X phosphate-buffered saline, pH 7.4 (PBS). A total of 10 samples were prepared (Table 2). The tissues were fully submerged in the LNC suspensions to ensure the

efficient interaction between the DiD-loaded LNCs and the tissue. The tissue were incubated with the DiD-loaded LNC suspensions for 10 days, without stirring, at 37°C.

Aliquots of 50 µL were collected from each sample on day 0, day 3, day 5, and day 10. Subsequently, after the desired incubation period of day 10, the samples were diluted to a concentration of 0.4 mg/ml to quantify the extent of LNCs uptake or interaction with the tissue using fluorescence spectroscopy. The fluorescence spectra were measured using a FluoroMax®-4 (Horiba Scientific, New Jersey, USA) with an excitation wavelength of 445 nm. Maximal intensity corresponded to an emission wavelength of 665 nm. Furthermore, linear titration curves (R^2 = 0.9991, 0.9993 and, 0.9995) for DiD-loaded LNCs with Span compositions of 0, 0.14 and 0.27 (w/w_{LNC}), were observed, by diluting the LNC suspensions after the formulation process, in PBS to achieve concentrations from 0.05 to 0.7 mg/ml.

2.5 Statistics

Results are expressed as the mean ± standard deviation (SD) of six independent experiments for characterization of LNCs and one for *ex vivo* experiment. Statistical analyses were performed using GraphPad Prism (GraphPad Software, USA). The data were evaluated using the one-way ANOVA statistical test. A p-value lower than 0.05 was considered statistically significant.

3 Results and discussion

3.1 Characterization of LNCs with various Span compositions

The characterization of LNCs with various Span compositions of 0, 0.14 and 0.27 (w/w_{LNC}) provided a comprehensive understanding of the size and morphology by determining the average size, size distribution, and surface charge of LNCs analyzed by the dynamic light scattering (DLS) technique (Figure 1A). These parameters provided valuable information about the physical properties and stability of LNCs. The average size of LNCs is a critical parameter in determining their behavior and functionality. DLS measured the intensity fluctuations of scattered light caused by the Brownian motion of particles suspended in a solution. From these fluctuations, the hydrodynamic diameter of the particles was calculated, and all three formulations showed an average size from 50 to 60 nm which indicated good repeatability of the preparation method of LNC formulations. The average size of LNCs obtained through DLS showed the effective diameter of the particles, including the lipid core and the surrounding surfactant layer (Figure 1B). Additionally, the size of LNCs could influence their circulation time and penetration into tissues.

PdI is a measure of the size distribution or heterogeneity of nanoparticles. It provided information about the uniformity of the particle sizes within a sample. All the LNC formulations showed PdI values < 0.1 which indicates a monodisperse population and suggests homogenous and reproducible LNC formulations (Figure 1C). Zeta potential characterizes the surface charge of LNCs and is a measure of the electrostatic repulsion or attraction between particles in a solution. It is determined by the distribution of charged molecules or functional groups on the surface of the nanoparticles. Zeta potential was measured using electrophoretic mobility, which quantifies the movement of particles under the influence of an electric field to the LNC dispersion and monitors the resulting electrophoretic mobility of the particles. The magnitude and sign of the zeta potential indicated the degree of electrostatic repulsion or attraction between LNCs. All the prepared LNCs showed zeta potential < -6 mV may indicate a neutral surface of LNCs (Figure 1D). It also provides insights into the potential interactions between LNCs and biological components, such as cell membranes and proteins. By optimizing the zeta potential, LNCs with enhanced stability and desired interactions with the target site can be designed.

3.2 Internalization of LNCs into blood vessel ex vivo tissue

The blood vessel tissues were prepared and exposed to a solution containing different lipid nanocapsule formulations (Span composition of 0, 0.14, and 0.27 (w/w_{LNC}). The tissues were immersed in this solution and incubated for a specific period of 10 days to facilitate interaction between the tissues and LNCs. During the incubation period, the lipid nanocapsules came into contact with the blood vessel tissues, and their lipid bilayer interacted with the cell membranes of the tissues, promoting internalization. This process aimed to study the behavior and cellular interactions of the LNCs with tissues. The cumulative adsorption of LNCs in the tissues refers to the gradual accumulation or deposition of these nanocapsules within the tissues throughout the incubation period. Only the supernatant of 50 µL was removed from the samples, and the distribution of lipid nanocapsules within the biological media of the tissues was assessed through fluorescence measurements. This allowed for an evaluation of the overall uptake or accumulation of LNCs over time.

The LNC formulation with Span composition of 0 (w/w_{LNC}) exhibited a sudden increase in the adsorption of LNCs within the carotid artery of mice after just one day of incubation. By day 10 of incubation, the adsorption rate had reached 68%. Additionally, there was increased uptake of LNCs within the femoral artery of rats. However, the results for the femoral artery differed between days 5 and 10 of incubation, potentially due to the presence of fat constituents surrounding the artery, which may have affected the adsorption of LNCs. The highest internalization of LNCs on day 10 was observed in one of the femoral arteries of mice, reaching 73%. (Figure 2A).

After one day of incubation, the LNCs with Span composition of 0.14 (w/w_{LNC}) exhibited a consistent increase in internalization within the aorta and carotid of mice. The maximum internalization rate of LNCs reached 60% on day 10 of the incubation period

Table 1. Compositions of the formulations before the phase inversion formulation process for the preparation of lipid nanocapsule (LNC) suspensions.

Span composition (w/w_{LNC})			
Ingredient (g)	**0**	**0.14**	**0.27**
NaCl	0.054	0.054	0.054
Kol	1.367	1.067	0.767
Span	0	0.3	0.6
Lab	1.117	1.117	1.117
Water	1.517	1.517	1.517

Table 2. Incubation of different LNC formulations and arterial types obtained from mice and rats.

Formulations	Arteries
Span 0 (w/w_{LNC})	Femoral of rat
Span 0.14 (w/w_{LNC})	Aorta of mice
Span 0.27 (w/w_{LNC})	Carotid of mice
Span 0 (w/w_{LNC})	Carotid of mice
Span 0.14 (w/w_{LNC})	Carotid of mice

Formulations	Arteries
Span 0.27 (w/w_{LNC})	Carotid of mice
Span 0.27 (w/w_{LNC})	Carotid of mice
Span 0 (w/w_{LNC})	Femoral of rat
Span 0.14 (w/w_{LNC})	Carotid of rat
Span 0.27 (w/w_{LNC})	Carotid of rat

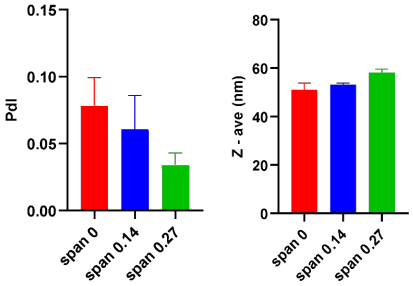

Various Span composition			
Parameters	**0**	**0.14**	**0.27**
Z-av (d.nm)	51 ± 3	53 ± 1	58 ± 1.5
PdI	0.08 ± 0.02	0.06 ± 0.03	0.03 ± 0.01
ZP (mV)	Neutral	Neutral	Neutral

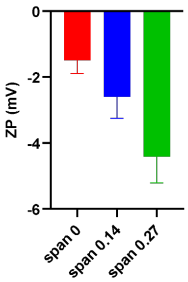

Figure 1. Size distribution (Z-average: Z-ave, and Polydispersity Index: PdI) and Zeta potential (ZP) of lipid nanocapsules (LNCs) in suspensions after their preparation thanks to the phase inversion formulation process (dilution factor 1:60 (v/v)) (n = 6; mean ± SD) (A-D).

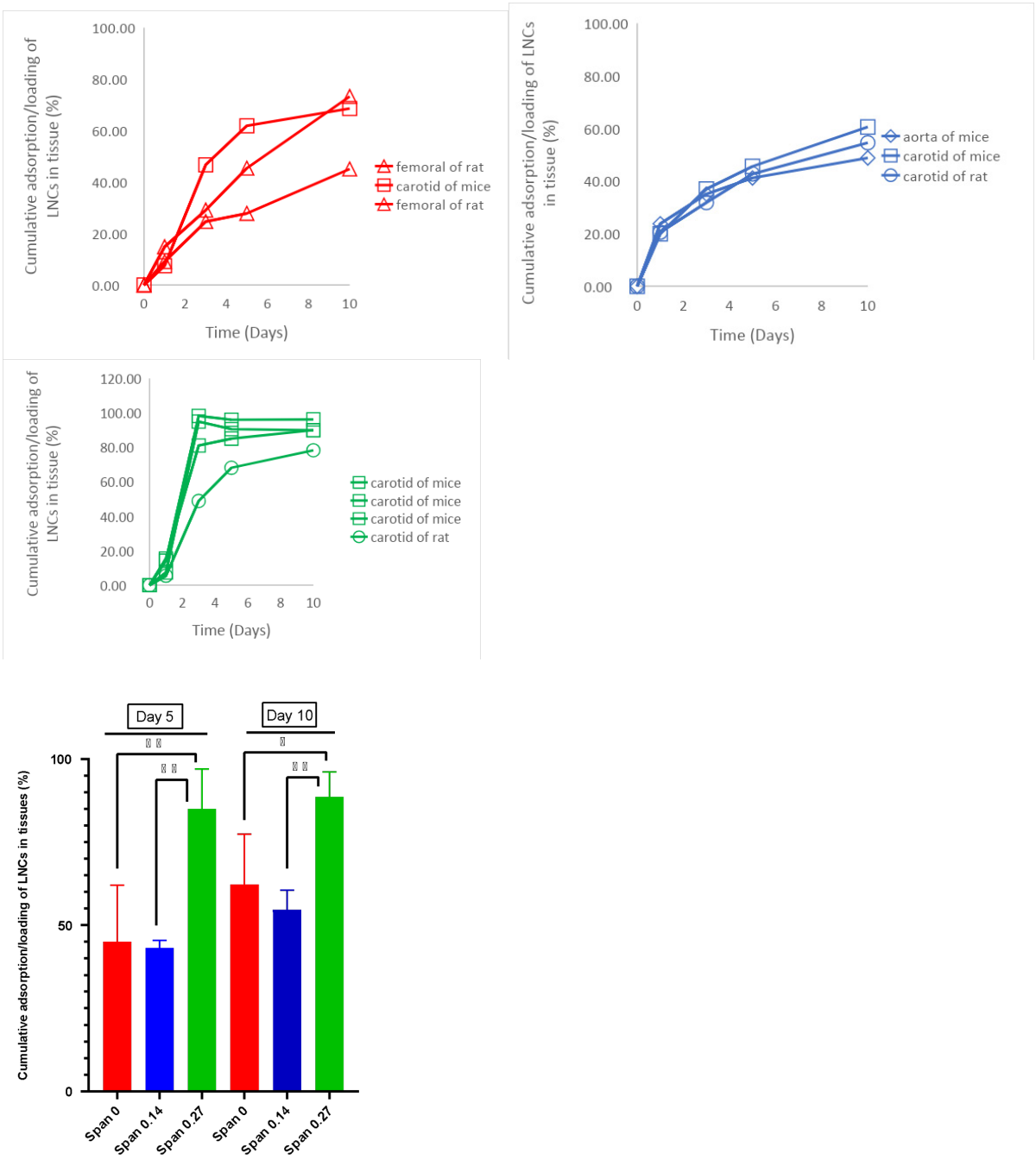

Figure 2. The fluorescence measurements quantified the cumulative adsorption/loading of LNCs in tissues (A-D). (□) carotid of mice, (Δ) femoral of rat, (○) carotid of rat, and (◇) aorta of mice (A-C). A) For Span composition 0 (w/w_{LNC}), the adsorption of LNCs in the given tissues was measured after incubation for 10 days, with samples collected on days 0, 1, 3, 5, and 10. B) For Span composition 0.14 (w/w_{LNC}), the adsorption of LNCs in the given tissues was measured after incubation for 10 days, with samples collected on days 0, 1, 3, 5, and 10. C) For Span composition 0.27 (w/w_{LNC}), the adsorption of LNCs in the given tissues was measured after incubation for 10 days, with samples collected on days 0, 1, 3, 5, and 10. D) The cumulative adsorption/loading of LNCs in tissues [%] was analyzed for Span composition 0 (w/w_{LNC}), (red profile), 0.14 (w/w_{LNC}), (blue profile), and 0.27 (w/w_{LNC}) (green profile) on day 5 and day 10. The results are presented as mean ± SD. The p-values are indicated in black (*) (* $p < 0.05$, ** $p < 0.01$).

(Figure 2B). On day 3 of incubation, the LNCs with Span composition of 0.27 (w/w_{LNC}) exhibited faster and more rapid adsorption into the carotid arteries of both mice and rats. After just three days of incubation, the internalization of LNCs reached high levels: 81%, 98%, and 94% in the carotid arteries of mice. However, in the carotid artery of the rat, the internalization rate was lower, around 48%, compared to these mentioned samples. This trend remained consistent for three of the carotid artery samples on both days 5 and 10 (Figure 2C). On days 5 and 10 of the incubation, it was demonstrated that there was a notable contrast between the LNCs with Span composition 0 and 0.27 (w/w_{LNC}), as well as between Span composition 0.14 and 0.27 (w/w_{LNC}) (Figure 2D).

The structure of Span (sorbitan monooleate) can play a crucial role in enhancing the internalization of LNCs within tissues. The formulation with Span composition 0.27 (w/w_{LNC}) showed high absorption into the tissue due to the increased sorbitol functions at the surface of the LNCs, interacting with specific receptor at the cell surface. This interaction can promote the fusion or adsorption of LNCs onto the cell membrane, facilitating their internalization through endocytosis or other cellular uptake mechanisms. Additionally, Span 80 possesses both hydrophilic and hydrophobic regions within its molecular structure. This amphiphilic nature can allow it to effectively interact with both the aqueous environment and the lipid components of LNCs. This interaction can help stabilize the LNCs and promote their internalization within tissues (Palazzo et al., 2016).

4 Conclusion and perspectives

In conclusion, this study focused on the development of lipid nanocapsules (LNCs) using the phase-inversion method and examined their surface properties by incorporating different concentrations of span 80. Our primary objective was to investigate the interaction between these LNC formulations and blood vessels in *ex vivo* tissues. Characterization of each LNC formulation was performed using dynamic light scattering (DLS), which provided valuable information about the size distribution and stability of the nanocapsules. This characterization step allowed us to assess the physical properties of the LNCs and ensure their suitability for subsequent interaction studies. Through *ex vivo* experiments, we were able to observe and analyze the interaction of the LNC formulations with blood vessels. By quantifying the cumulative adsorption/loading of the LNCs in different tissues, we gained insights into their behavior and potential for targeted drug delivery. The results of this study demonstrated that the surface properties of the LNCs, modulated by varying concentrations of span 80, influenced their interaction with blood vessels. This finding highlights the importance of surface engineering in optimizing the efficacy and specificity of nanocarriers for drug delivery applications. Overall, this research contributes to the understanding of LNC development and its interaction with blood vessels. The combination of phase-inversion synthesis, span 80 modification, and DLS characterization provides a comprehensive approach to tailoring LNC formulations for improved applications in cardiovascular pathologies. Future studies can further explore the *in vivo* behavior and therapeutic potential of these LNCs, paving the way for their translation into clinical practice.

Author contributions

S.N. formulated the study objectives, constructed the hypotheses, and revised the manuscript. G.B.P. conducted the literature review. P.S. was responsible for data collection and analysis. All authors reviewed and approved the final manuscript.

Acknowledgment

Author was grateful to their department.

Competing financial interests

The authors have no conflict of interest.

References

Béduneau, A., Saulnier, P., Hindré, F., Clavreul, A., Leroux, J.-C., & Benoit, J.-P. (2007). Design of targeted lipid nanocapsules by conjugation of whole antibodies and antibody Fab' fragments.Biomaterials,28(33), 498–4990. https://doi.org/10.1016/j.biomaterials.2007.05.014

Bhargava, B., Reddy, N. K., Karthikeyan, G., Raju, R., Mishra, S., Singh, S., Waksman, R., Virmani, R., & Somaraju, B. (2006). A novel paclitaxel-eluting porous carbon-carbon nanoparticle coated, nonpolymeric cobalt-chromium stent: Evaluation in a porcine model. Catheterization and Cardiovascular Interventions, 67(5), 698–702. https://doi.org/10.1002/ccd.20698

Brito, L., & Amiji, M. (2007). Nanoparticulate carriers for the treatment of coronary restenosis. International Journal of Nanomedicine, 2(2), 143–161. https://doi.org/10.2147/nano.2007.2.2.143

Chakraborty, S., Kar, S., & Mazumder, B. (2021). Disease-specific biomaterials for targeted drug delivery: Emerging needs, signals, and challenges. ACS Biomaterials Science & Engineering, 7(9), 4191–4224. https://doi.org/10.1021/acsbiomaterials.1c00623

Déglise, P., Nguyen, T. V., & Déglise, C. (2022). Intimal hyperplasia: Challenges and perspectives. Journal of Clinical Medicine, 11(1), 183. https://doi.org/10.3390/jcm11010183

Farb, A., Sangiorgi, G., Carter, A. J., Walley, V. M., Edwards, W. D., Schwartz, R. S., & Virmani, R. (2002). Pathology of acute and chronic coronary stenting in humans. Circulation, 99(1), 44–52. https://doi.org/10.1161/01.cir.99.1.44

Fowkes, F. G. R., Rudan, D., Rudan, I., Aboyans, V., Denenberg, J. O., McDermott, M. M., Norman, P. E., Sampson, U. K., Williams, L. J., Mensah, G. A., & Criqui, M. H. (2013). Comparison of global estimates of prevalence and risk factors for peripheral artery disease in 2000 and 2010: A systematic review and analysis. The Lancet, 382(9901), 1329–1340. https://doi.org/10.1016/S0140-6736(13)61249-0

Groo, A.-C., Saulnier, P., & Gimel, J.-C. (2018). Understanding the adsorption mechanism of monoclonal antibodies on lipid nanocapsules: Toward targeted nanomedicines. Langmuir, 34(33), 9837–9846. https://doi.org/10.1021/acs.langmuir.8b01547

Heurtault, B., Saulnier, P., Pech, B., Proust, J. E., & Benoit, J. P. (2002). A novel phase inversion-based process for the preparation of lipid nanocarriers. Pharmaceutical Research, 19(6), 875–880. https://doi.org/10.1023/A:1016121319668

Hirsjärvi, S., Sancey, L., Dufort, S., Belloche, C., Vanpouille-Box, C., Garcion, E., Coll, J. L., Hurbin, A., & Benoit, J. P. (2012). Effect of particle size on the biodistribution of lipid nanocapsules: Comparison between nuclear and fluorescence imaging and counting. International Journal of Pharmaceutics, 438(1–2), 107–115. https://doi.org/10.1016/j.ijpharm.2012.08.028

Huynh, N. T., Roger, E., Lautram, N., Benoit, J. P., & Saulnier, P. (2009). The rise and rise of lipid nanocapsules as multifaceted nanomedicines. Therapeutic Delivery, 1(4), 435–456. https://doi.org/10.4155/tde.10.19

Li, J., Wang, Y., Liang, R., Chen, J., & Zhang, H. (2016). Recent advances in targeted nanoparticles drug delivery to melanoma. Nanomedicine, 12(5), 1239–1255. https://doi.org/10.1016/j.nano.2016.01.017

Matougui, N., Boge, L., Groo, A. C., Umerska, A., Pellequer, Y., Ringstad, L., Bysell, H., & Saulnier, P. (2016). Nanoparticles designed for overcoming the mucus barrier for oral delivery of calcitonin. International Journal of Pharmaceutics, 500(1–2), 63–72. https://doi.org/10.1016/j.ijpharm.2015.12.046

Melnik, E., Konevega, L., Stupin, V., & Konstantinova, E. (2022). Intimal hyperplasia in vascular grafts: The role of surface microstructure. International Journal of Molecular Sciences, 23(19), 11238. https://doi.org/10.3390/ijms231911238

Minkov, I., Miroux, A., Giacometti, S., Müller, M., Lehmann, L., Proust, J. E., & Grossiord, J. L. (2005). Biocompatible surfactant-free preparation of liposomes, polymersomes, and lipid nanocapsules. Journal of Colloid and Interface Science, 284(1), 228–237. https://doi.org/10.1016/j.jcis.2004.10.048

Mylonaki, I., Allara, E., Chocron, S., Dubourg, Q., Alcazar, D. P., Trimaille, A., Katsiki, N., Blomberg, A., & Giral, P. (2018). Direct and indirect comparison of the effects of antihypertensive drugs on atherosclerosis and intima-media thickness: A systematic review and network meta-analysis. Journal of Clinical Hypertension, 20(11), 1501–1508. https://doi.org/10.1111/jch.13469

Nemenoff, R. A., Simpson, P. A., Furgeson, S. B., Kaplan-Albuquerque, N., Crossno, J., Garl, P., & Offermanns, S. (2008). The role of RhoA and Rho kinase in vascular smooth muscle cell proliferation. Vascular Pharmacology, 48(2–3), 50–57. https://doi.org/10.1016/j.vph.2007.10.009

Palazzo, C., Karim, R., Evrard, B., & Piel, G. (2016). Drug delivery nanocarriers to cross the blood-brain barrier. In Drug delivery across the blood-brain barrier (pp. 1-22). Elsevier. https://doi.org/10.1016/B978-0-323-42866-8.00001-0

Saulnier, P., Benoit, J.-P., & Heurtault, B. (2002). Design and characterization of lipid nanocapsules. Pharmaceutical Research, 19(6), 875–880. https://doi.org/10.1023/A:1016121319668

Umerska, A., Mouzouvi, C. R., Bigot, A., Saulnier, P., & Costantino, H. R. (2015). Polymeric nanoparticles for increasing oral bioavailability of a poorly water-soluble drug: Effect of particle size and crystalline state on solubility and dissolution rate. International Journal of Pharmaceutics, 494(1), 211–220. https://doi.org/10.1016/j.ijpharm.2015.08.062

Urimi, D., Patel, S. R., Patel, P. P., & Patel, B. R. (2021). Lipid nanoparticles: An innovative technique for drug delivery systems. Materials Today: Proceedings, 50, 1429–1435. https://doi.org/10.1016/j.matpr.2021.09.267

Westedt, U., Steinhäuser, I., & Kissel, T. (2002). Influence of process parameters on preparation of loperamide-loaded poly(lactic-co-glycolic acid) nanoparticles: A factorial design study. International Journal of Pharmaceutics, 232(1–2), 101–112. https://doi.org/10.1016/s0378-5173(01)00922-7